Special Issue: International Conference on Contemporary Issues 2022
MJSAT 2 (S1) 16-21, December 2022

MJSAT

Malaysian Journal of Science and Advanced Technology

journal homepage: https://mjsat.com.my/

Study of Bio-Fluid Dynamics in Carotid Artery System Using Numerical Methods

R Shenoy [1], H N Abhilash [2], A A Basri [3], A B V Barboza [2], G Shenoy B[2], R Pai [2] and S M A Khader *[2]

[1]*Dept. of Mechanical Engineering, School of Science and Engineering, Manipal International University. Nilai, Malaysia.*
[2]*Dept. of Mechanical & Industrial Engineering, Manipal Institute of Technology, Manipal Academy of Higher Education, Manipal, India.*
[3]*Dept. Aerospace Engineering, Universiti Putra Malaysia, Selangor, Malaysia.*

KEYWORDS

Carotid Artery
Atherosclerosis
Haemodynamics
Helicity

ABSTRACT

Computational Fluid Dynamics (CFD) has been largely used in understanding the haemodynamics of the carotid bifurcation system and to visualise the blood flow changes due to the carotid artery geometric variations. Such studies will be helpful in understanding the arterial blood flow behavior and atherosclerosis. The present study focuses on investigation of geometric variable patient-specific healthy carotid bifurcation system under physiological pressure conditions. Unsteady flow simulation is conducted in ANSYS Fluent under the rigid wall and non-Newtonian conditions. The haemodynamic parameters such as pressure, velocity, vorticity, helicity, and time-averaged wall shear stress (TAWSS) were evaluated to visualise and understand flow dynamics at critical zones of bifurcation system. Further, the importance of geometric influence on the bifurcation zone was also investigated, causing significant vortex formation zones. A considerable reduction in velocity and backflow formation was observed, which is responsible for reducing the shear stress. It is also demonstrated that low TAWSS regions surrounding the bifurcation zone are more prone to atherosclerosis development.

1. INTRODUCTION

Cardiovascular diseases are one of the major contributors to global mortality [1]. Such diseases are primarily caused by an obstruction of blood flow due to narrowing of artery widely known as atherosclerosis [2, 3]. These diseases generally affect the medium and large size arteries due to build-up of fatty deposits on the inner walls of the artery [4]. The blood flow in normal and healthy artery gets significantly altered due to atherosclerosis [5]. Further, the atherosclerosis gets intensified affecting the normal blood circulation. These arterial diseases described by reducing of lumen diameter of artery resulting in flow obstruction thus severely reducing the blood flow to downstream organs [6]. The detailed study of the artery's gradual narrowing or bulging will help understand the underlying mechanisms for the unusual blood flow behavior. Haemodynamics study pertaining to large artery will be widely beneficial in the diagnosing and treating vascular diseases. Clinically analysing the haemodynamics will not benefit the exhaustive study with radiology imaging tools such as Digital angiography, Computer Tomography, Magnetic Resonance and Ultrasound duplex scanning [7]. The required haemodynamics data through numerical simulations results in better flow visualization. It is also observed that flow dynamics in the carotid artery is significantly affected by anatomical geometry and flow conditions. Later, such flow affected regions show relatively low wall shear stress and resulting in plaque development and progression [8, 9].

However, with the increasing trend of better computational capability, numerical methods are cheaper, valuable and extremely efficient substitute source for several researchers to in domain of bio fluid dynamics as compared to expensive experimental techniques [10, 11]. The numerical approach using CFD has been extensively practiced in the biofluid dynamics in virtue of lower computational cost [12, 13]. Besides, the analysis of haemodynamics, the importance of

*Corresponding author:
E-mail address: S M A Khader <smak.quadri@manipal.edu>.

anatomical geometric accuracy has to be established. The combination of numerical techniques with anatomically realistic geometry has become the current trend which uplifts the haemodynamics study closer to the actual conditions [14]. This approach certainly allows estimation of haemodynamics parameters such as wall shear stress indicating the initiation and progression of atherosclerosis [15]. The results obtained from such accurate patient specific geometries have claimed to influence the haemodynamics and physiological behavior of blood flow along the artery resulting in flow recirculation, local shear stresses and unidirectional flow. It is well established that anatomically realistic geometry strongly influences the of haemodynamic analysis and largely depends on the model configuration [16].

The literature review finds that the majority of the analysis considers patient specific case. However, there are limited flow dynamics studies that consider the effect of geometric variation of artery which is clinically very significant, since the substantial flow changes occurs at crucial geometric region and prone to atherosclerotic formation [17,18,19]. The present study considers anatomically different three carotid artery geometries for the investigation of haemodynamics at physiological blood pressures to prognosis for critical factors.

2. METHODOLOGY

2.1 Theory

The blood flow in the current vascular study is found to be to be non-Newtonian, incompressible and laminar [5, 8, 12]. The blood flow behavior is assumed to be laminar as it is considered under resting time of the cardiac cycle [20]. The Navier-Stokes governing equation adopted in the present study is show in equation (1) and (2) [21]. The Carreau Yasuda model is considered for non-Newtonian assumption which can solve the shear thinning and thickening fluid issues by combining Newtonian and Power-law models. The equation for effective viscosity for the Carreau Yasuda model is described by equation 3 [22].

$$\nabla . \upsilon = 0 \qquad (1)$$

$$\rho\left(\frac{d\upsilon}{dt} + \upsilon . \nabla \upsilon\right) = -\nabla p + \mu \nabla^2 \upsilon \qquad (2)$$

$$\eta(\gamma) = \mu_\infty + (\mu_0 - \mu_\infty)[1 + (\lambda\dot{\gamma})^a]^{\frac{n-1}{a}} \qquad (3)$$

Where γ is the shear rate, η is the viscosity, μ_0 is the viscosity at zero shear rate, μ_∞ is the viscosity at infinite shear rate, λ, α, and n are material coefficients (λ = 1.902 s, α = 1.25, n = 0.22), a is Yasuda constant (a=1.25).

2.2 Modelling

The present study focuses on three different geometric shape subject-specific carotid bifurcation models for comparing the haemodynamic investigation as shown in Figure 1. A typical carotid system consists of Common Carotid Artery (CCA)bifurcating into External Carotid Artery (ECA) and Internal Carotid Artery (ICA). A three-dimensional patient-specific model was created from CT-Angio data post-reconstruction using MIMICS 19 (Materialise, Leuven, Belgium) medical image processing software. Geometry construction steps are referred from literature [5,6]. The carotid bifurcation models/cases (a, b and c) were discretized using polyhedral elements. Hybrid mesh is generated using Fluent meshing module wherein the mesh along the boundary wall contains octahedral elements and the interior is made up of hexahedral elements. The grid independence tests were carried out for all three models considering peak values for velocity inlet and pressure outlet. Change in velocity is monitored for change in grid size at CCA, ECA and ICA. The grid test evaluation finds that velocity and pressure are normalized with the number of elements 420000 for case-a, 390000 for case-b, and 410000 for case-c. [12,19]. In the current study, μ_∞ and μ_0 is considered to be 0.00345 Pas and 0.056 Pas respectively as found in equation 3.

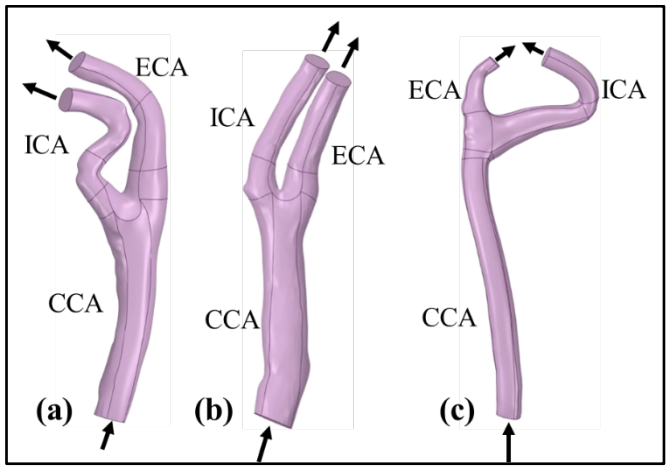

Fig. 1. Geometric models of various carotid bifurcation

2.3 Analysis

Unsteady pulsatile flow velocity is defined at the inlet with a cardiac cycle of 0.8s as shown in Figure 2. Physiological pulsatile pressure waveform is applied at the outlet faces as described in Figure 3. These time varying pulsatile waveforms were applied at the inlet and the outlet region through user-defined function, however the walls of the models were assumed to be rigid [14,15,16]. Resistance type boundary condition is adopted at the outlet considering peripheral resistance under physiological conditions. The methodology of inlet and outlet pulse wave generation is similar to that adopted in literature [4,20]. Pulsatile waveforms of velocity and pressure wave were divided into 180-time steps to capture flow behavior more precisely [21,22]. The timestep independence has been conducted and each time step of 0.005 seconds for total 180-time steps is adopted to capture the flow behavior. Convergence criteria of $1x10^{-5}$ was set during unsteady simulation [19,20].

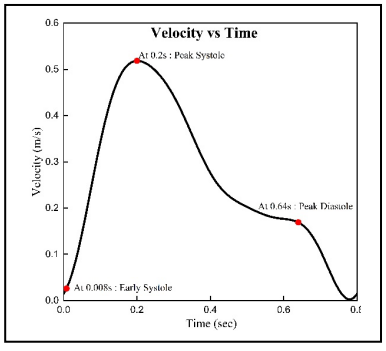

Fig. 2. Inlet pulsatile velocity wave form

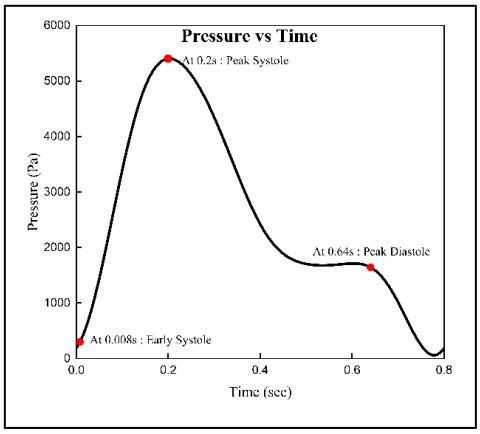

Fig. 3. Outlet pulsatile pressure wave form

3. RESULTS AND DISCUSSIONS

The results of the unsteady blood flow CFD analysis are compared for various geometric models. The cardiac cycle consists of three specific phases; early systole (0.06s), peak systole (0.22s), and peak diastole (0.44s) were considered to evaluate the haemodynamic factors like velocity, pressure, time-averaged wall shear stress, vorticity and helicity are that compared among three carotid artery models. The flow rate of 70/30 distribution has been observed which represents the upper physiological flow ratio between the ICA and ECA. The peak systole time instant has been considered to describe and discuss the results obtained as maximum changes occurs during this instant of cardiac cycle.

3.1 Velocity

Flow variation at the bifurcation region is captured in different models in the form of velocity streamlines. Velocity streamlines are shown in Figure 4. The ECA of case (b) and (c) are similar in geometric nature in contrast to case (a) which is highly tortuous which is evident from the velocity behavior profile. The CCA profile is straight in all three carotid models and has similar velocity behavior. In all three cases, the flow is characterized by a steep velocity gradient at the bifurcation region and stagnant/reversed flow along the outer wall of the ICA. Because of the different geometric profiles of ICA branching in three models, the flow velocity is higher in ICA than in ECA in case (b) and (c), while in case (c), the flow is equally distributed with slightly higher magnitude in ICA than in ECA. Due to the higher curvature of ICA than ECA in bifurcation models, the flow separation occurs mainly in the outer wall of ICA with the increased flow towards the inner wall of ICA as clinically observed [12,22,23]. At peak systole along the center line of geometry, 50% magnitude of peak velocity value is observed in CCA of all three models. However, due to velocity gradients recirculation zones were observed in case (c) near the outer wall of ECA. It is observed that in all three cases towards the inner wall of ECA, flow is aligned to the geometry of the artery. In ICA due to curvature case (a) velocity streamlines are tortuous, whereas in the case of case (b) & (c) having streamlines aligned to geometry during peak systole. During early diastole, CCA observed streamline flow until the bifurcation in case (c), whereas case (a) & (b) had recirculation near the inner wall and outer wall zones respectively due to steep velocity gradients. The case of ECA in case (a) has streamline flow whereas case (b) and (c) have twisting streamlines along with the geometry during early diastole [22, 23]. However, the flow in ICA of case (a) is disturbed due to curvature, whereas case (b) and case (c) observed geometry aligned flow with maximum velocity near the inner wall.

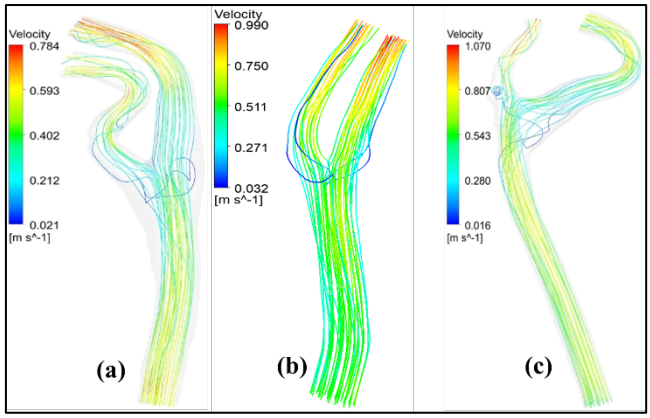

Fig. 4. Comparison of velocity streamlines in different carotid bifurcation system

3.2 Pressure

The pressure contours of all the three cases are shown in Figure 5. The distribution of pressure is however not uniform in all three cases especially at bifurcation zone. Further, it is also observed that along the length of the straight portion of CCA, the circumferential pressure distribution is uniform whereas at curved locations it varied significantly along with ECA and ICA during peak systole [24]. In all the three cases, minimum pressure at ECA and ICA outlets have been observed. However, in case-(a) whereas maximum pressure was observed in the inner wall of bifurcation. In case-(b) along the length of CCA and ECA the pressure distribution is observed to be in a range with magnitude varying near mean pressure value. Also, in case-(c) the maximum pressure is at the inner wall of bifurcation and at the origin of ECA the pressure distribution is slightly large. Along the length of ECA, CCA, and ICA pressure distribution is not uniform [25]. During the entire, pulse cycle, the location of max pressure remains to be the inner wall of bifurcation and minimum pressure at the outlets of ICA and ECA.

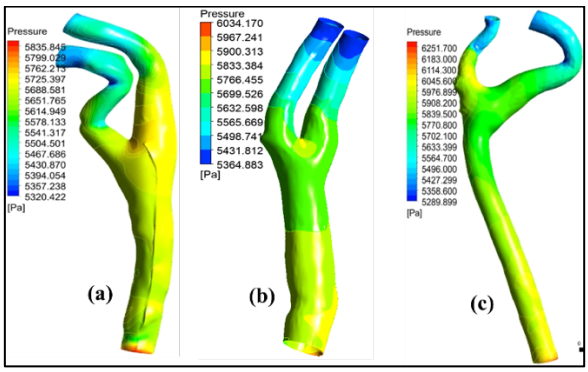

Fig. 5. Pressure contour comparison in different carotid bifurcation system

3.3 Helicity

Figure 6 depicts the isosurface of helicity patterns signifying the positive and negative flows in the carotid artery bifurcation system. Generally, the intravascular flow profile within the carotid bifurcation system is particularly characterized by a helical pattern. The helical flow patterns are visualized by setting a threshold of ± 1. The negative values represent counter clockwise flow whereas the positive represent clockwise, the values near zero show lesser helical intensities [24,25]. The low-intensity helicity begins at the flow divider region of bifurcation zone and later develops fully into the sinus region in the ICA. The observations are similar for all the carotid cases qualitatively, however, there exists few flow reversal changes during later part of cardiac cycle [7,19,26]. Regions having lesser helical intensity seemingly start from the sinus and intensified in the lower ICA. Also, the patterns of low helical intensity are distributed to a larger surface during early diastole in all the three cases.

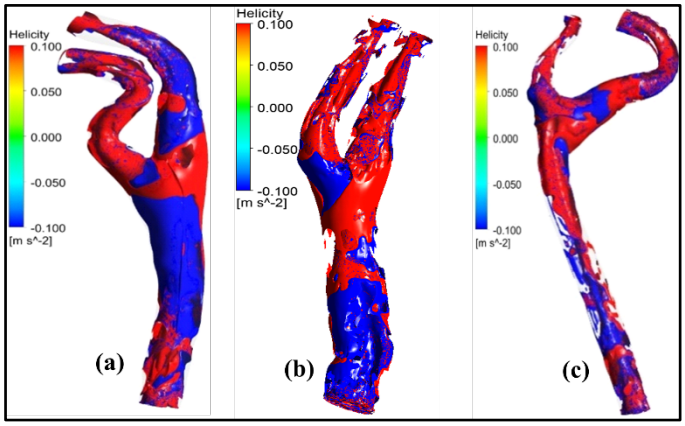

Fig. 6. Helicity plots in various carotid bifurcation system

3.4 Vorticity

The vorticity contours in carotid artery models as shown in the Figure 7. The evaluation of vorticity has prime importance in understanding the flow patterns of arterial blood flow system. The development of three-dimensional secondary flow fields influences the flow near to the wall. The fluid flow along the axis perpendicular to the wall generates pressure gradients in its surrounding area [17,24]. In all the three carotid cases, the boundary layer upstream of CCA undergoes three-dimensional flow separation as seen in the Figure 6. The flow recirculates downstream of the separation line for a vortex zone. As the flow approaches the apex of the bifurcation zone, it deviates into reverse directions perpendicular to its actual path, demonstrating vortex formation. Therefore, it was observed that the flow separation occurs at the lateral wall of the ICA at the apex at the corner where the ECA is branching in all the carotid cases.

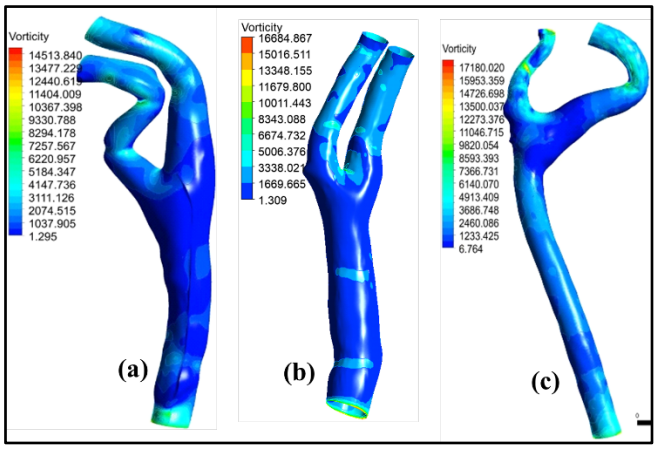

Fig. 7. Vorticity plots description in different carotid bifurcation system

3.5 Time Average Wall Shear Stress (TWSS)

The variation of WSS throughout a cardiac cycle can be determined using TAWSS and is described as shown in the Figure 8. It is well known that atherosclerosis is more likely to develop in areas with low TAWSS values [27,28]. In case (a) during early diastole, the region or surface area having a low range of TAWSS is greater when compared to peak systole. This behavior implies that blood flow during early diastole has less value of TAWSS resulting in progression of atherosclerosis. However, in case (b) and (c), the peak systole has a larger surface area with less TAWSS when compared to early diastole. In case 1, a region with less TAWSS is located closer to the bifurcation region especially towards ECA. However, in case (b) and (c), location of less TAWSS is towards ICA in bifurcation region. Hence, it is clearly demonstrated that geometric profile of the carotid artery plays a major role in understanding the haemodynamics of the artery. The TAWSS is a temporal average of the WSS over a full cardiac cycle.

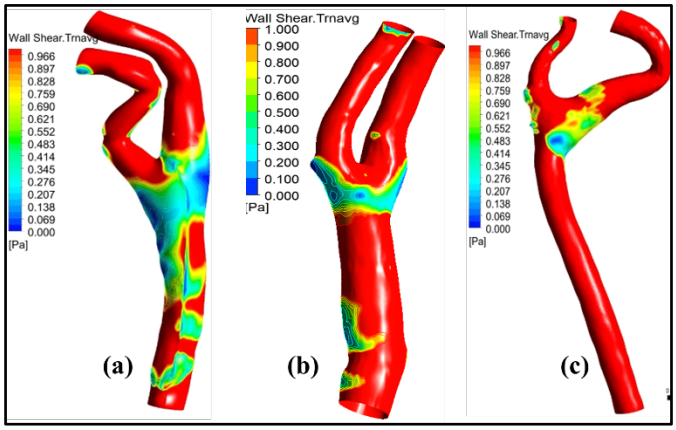

Fig. 8. TWSS comparison in different carotid bifurcation system

4. CONCLUSION

The different geometric shapes of the carotid bifurcation system are numerically investigated in the current study under

physiological conditions. Haemodynamic parameters such as velocity, pressure, helicity, vorticity, and time-averaged wall shear stress have been evaluated and discussed. Due to the different geometric profiles of ICA branching in all the three models, higher flow is observed in ICA in contrast to ECA flow distribution. The steep velocity gradient at the bifurcation region and reversed flow patterns along the outer wall of ICA are significantly demonstrated in all three models. Further, there is a qualitative behavior of helicity and vorticity in the bifurcation region. Significance of vortex formation has demonstrated in all the models when the flow approaches the apex of bifurcation and later diverges into reverse directions to the initial path. It is established that atherosclerosis is more likely to develop in areas with low TAWSS values especially spread to larger surface during peak systole. Moreover, it is verified that the bifurcation region plays a vital role in flow dynamics of the artery. This study can be further extended by considering the influence of elastic artery and stenosed cases.

ACKNOWLEDGEMENT

This work is Department of Radio-Diagnosis and Imagining, Kasturba Medical College, Manipal for providing the patient specific data on carotid artery.

REFERENCES

[1] Reddy, K. Srinath. "Cardiovascular diseases in the developing countries: dimensions, determinants, dynamics and directions for public health action." Public health nutrition 5, no. 1a (2002): 231-237. https://doi.org/10.1079/PHN2001298

[2] Subramaniam, Thineshwaran, and Mohammad Rasidi Rasani. "Pulsatile CFD Numerical Simulation to investigate the effect of various degree and position of stenosis on carotid artery hemodynamics." Journal of Advanced Research in Applied Sciences and Engineering Technology 26, no. 2 (2022): 29-40.

[3] Ramdan, Salman Aslam, Mohammad Rasidi Rasani, Thinesh Subramaniam, Ahmad Sobri Muda, Ahmad Fazli Abdul Aziz, Tuan Mohammad Yusoff Shah Tuan Ya, Hazim Moria, Mohd Faizal Mat Tahir, and Mohd Zaki Nuawi. "Blood Flow Acoustics in Carotid Artery." Journal of Advanced Research in Fluid Mechanics and Thermal Sciences 94, no. 1 (2022): 28-44.

[4] Perktold, Karl, and Gerhard Rappitsch. "Computer simulation of local blood flow and vessel mechanics in a compliant carotid artery bifurcation model." Journal of biomechanics 28, no. 7 (1995): 845-856.

[5] Hegde, Pranav, A. B. V. Barboza, SM Abdul Khader, Raghuvir Pai, Masaaki Tamagawa, Ravindra Prabhu, and D. Srikanth Rao. "Numerical Analysis on A Non-Critical Stenosis in Renal Artery." Journal of Advanced Research in Fluid Mechanics and Thermal Sciences 88, no. 3 (2021): 31-48.

[6] Al-Azawy, Mohammed Ghalib, Saleem Khalefa Kadhim, and Azzam Sabah Hameed. "Newtonian and non-newtonian blood rheology inside a model of stenosis." CFD Letters 12, no. 11 (2020): 27-36.

[7] Zain, Norliza Mohd, Zuhaila Ismail, and Peter Johnston. "A Stabilized Finite Element Formulation of Non-Newtonian Fluid Model of Blood Flow in A Bifurcated Channel with Overlapping Stenosis." Journal of Advanced Research in Fluid Mechanics and Thermal Sciences 88, no. 1 (2021): 126-139.

[8] Torii, Ryo, Marie Oshima, Toshio Kobayashi, Kiyoshi Takagi, and Tayfun E. Tezduyar. "Fluid–structure interaction modeling of aneurysmal conditions with high and normal blood pressures." Computational Mechanics 38, no. 4 (2006): 482-490.

[9] Fu, Yulin, Aike Qiao, and Long Jin. "The influence of hemodynamics on the ulceration plaques of carotid artery stenosis." Journal of Mechanics in Medicine and Biology 15, no. 01 (2015): 1550008.

[10] Li, Cong-Hui, Bu-Lang Gao, Ji-Wei Wang, Jian-Feng Liu, Hui Li, and Song-Tao Yang. "Hemodynamic factors affecting carotid sinus atherosclerotic stenosis." World Neurosurgery 121 (2019): e262-e276.

[11] Gallo, Diego, David A. Steinman, Payam B. Bijari, and Umberto Morbiducci. "Helical flow in carotid bifurcation as surrogate marker of exposure to disturbed shear." Journal of biomechanics 45, no. 14 (2012): 2398-2404.

[12] Lim, Sheh Hong, Mohd Azrul Hisham Mohd Adib, Mohd Shafie Abdullah, Nur Hartini Mohd Taib, Radhiana Hassan, and Azian Abd Aziz. "Study of extracted geometry effect on patient-specific cerebral aneurysm model with different threshold coefficient (Cthres)." CFD Letters 12, no. 10 (2020): 1-14.

[13] Gallo, Diego, David A. Steinman, and Umberto Morbiducci. "Insights into the co-localization of magnitude-based versus direction-based indicators of disturbed shear at the carotid bifurcation." Journal of biomechanics 49, no. 12 (2016): 2413-2419.

[14] Urevc, Janez, Iztok Žun, Milan Brumen, and Boris Štok. "Modeling the effect of red blood cells deformability on blood flow conditions in human carotid artery bifurcation." Journal of Biomechanical Engineering 139, no. 1 (2017): 011011.

[15] Campbell, Ian C., Jared Ries, Saurabh S. Dhawan, Arshed A. Quyyumi, W. Robert Taylor, and John N. Oshinski. "Effect of inlet velocity profiles on patient-specific computational fluid dynamics simulations of the carotid bifurcation." Journal of biomechanical engineering 134, no. 5 (2012).

[16] Morbiducci, Umberto, Diego Gallo, Diana Massai, Filippo Consolo, Raffaele Ponzini, Luca Antiga, Cristina Bignardi, Marco A. Deriu, and Alberto Redaelli. "Outflow conditions for image-based hemodynamic models of the carotid bifurcation: implications for indicators of abnormal flow." Journal of biomechanical engineering 132, no. 9 (2010).

[17] Bevan, Rhodri, P. Nithiarasu, Igor Sazonov, Raoul van Loon, Heyman Luckraz, Michael Collins, and Andrew Garnham. "Influences of domain extensions to a moderately stenosed patient-specific carotid bifurcation: Investigation of wall quantities." International Journal of Numerical Methods for Heat & Fluid Flow (2011).

[18] Hegde, Pranav, SM Abdul Khader, Raghuvir Pai, Masaaki Tamagawa, Ravindra Prabhu, Nitesh Kumar, and Kamarul Arifin Ahmad. "CFD Analysis on Effect of Angulation in A Healthy Abdominal Aorta-Renal Artery Junction." Journal of Advanced Research in Fluid Mechanics and Thermal Sciences 88, no. 1 (2021): 149-165.

[19] Sousa, Luísa C., Catarina F. Castro, Carlos C. António, Fernando Sousa, Rosa Santos, Pedro Castro, and Elsa Azevedo. "Computational simulation of carotid stenosis and flow dynamics based on patient ultrasound data–A new tool for risk assessment and surgical planning." Advances in medical sciences 61, no. 1 (2016): 32-39.

[20] Algabri, Yousif A., Surapong Chatpun, and Ishkrizat Taib. "An investigation of pulsatile blood flow in an angulated neck of abdominal aortic aneurysm using computational fluid dynamics." Journal of Advanced Research in Fluid Mechanics and Thermal Sciences 57, no. 2 (2019): 265-274.

[21] Paisal, Muhammad Sufyan Amir, Ishkrizat Taib, Ahmad Mubarak Tajul Arifin, and Nofrizalidris Darlis. "An analysis of blood pressure waveform using windkessel model for normotensive and hypertensive conditions in carotid artery." Journal of Advanced Research in Fluid Mechanics and Thermal Sciences 57, no. 1 (2019): 69-85.

[22] Bit, Arindam, Dushali Ghagare, Albert A. Rizvanov, and Himadri Chattopadhyay. "Assessment of influences of stenoses in right carotid artery on left carotid artery using wall stress marker." BioMed Research International 2017 (2017).

[23] Bruno, G., and C. Vergara. "Computational comparison between Newtonian and non-Newtonian blood rheologies in stenotic vessels''. Biomedical Technology." (2018): 169-183.

[24] Lee, Seung E., Sang-Wook Lee, Paul F. Fischer, Hisham S. Bassiouny, and Francis Loth. "Direct numerical simulation of transitional flow in a stenosed carotid bifurcation." Journal of biomechanics 41, no. 11 (2008): 2551-2561.

[25] Rayz, Vitaliy L., Stanley A. Berger, and David Saloner. "Transitional flows in arterial fluid dynamics." Computer methods in applied mechanics and engineering 196, no. 31-32 (2007): 3043-3048.

[26] Harrison, Gareth J., Thien V. How, Robert J. Poole, John A. Brennan, Jagjeeth B. Naik, S. Rao Vallabhaneni, and Robert K. Fisher. "Closure

technique after carotid endarterectomy influences local hemodynamics." Journal of Vascular Surgery 60, no. 2 (2014): 418-427.

[27] Kumar, Nitesh, Abdul Khader, Raghuvir Pai, Panayiotis Kyriacou, Sanowar Khan, and Prakashini Koteshwara. "Computational fluid dynamic study on effect of Carreau-Yasuda and Newtonian blood viscosity models on hemodynamic parameters." Journal of Computational Methods in Sciences and Engineering 19, no. 2 (2019): 465-477.

[28] Massai, Diana, Giulia Soloperto, Diego Gallo, Xiao Yun Xu, and Umberto Morbiducci. "Shear-induced platelet activation and its relationship with blood flow topology in a numerical model of stenosed carotid bifurcation." European Journal of Mechanics-B/Fluids 35 (2012): 92-101.